Quantum Nonlinear Optics with a Germanium-Vacancy Color Center in a Nanoscale Diamond Waveguide

M. K. Bhaskar,[1,*] D. D. Sukachev,[1,2] A. Sipahigil,[1] R. E. Evans,[1] M. J. Burek,[3] C. T. Nguyen,[1] L. J. Rogers,[4] P. Siyushev,[4] M. H. Metsch,[4] H. Park,[5] F. Jelezko,[4] M. Lončar,[3] and M. D. Lukin[1,†]

[1]*Department of Physics, Harvard University, 17 Oxford Street, Cambridge, Massachusetts 02138, USA*
[2]*P. N. Lebedev Physical Institute of the RAS, Leninsky Prospekt 53, Moscow 119991, Russia*
[3]*John A. Paulson School of Engineering and Applied Sciences, Harvard University, 29 Oxford Street, Cambridge, Massachusetts 02138, USA*
[4]*Institute for Quantum Optics, University Ulm, Albert-Einstein-Allee 11, 89081 Ulm, Germany*
[5]*Department of Chemistry and Chemical Biology, Harvard University, 12 Oxford Street, Cambridge, Massachusetts 02138, USA*

(Received 12 December 2016; published 31 May 2017)

We demonstrate a quantum nanophotonics platform based on germanium-vacancy (GeV) color centers in fiber-coupled diamond nanophotonic waveguides. We show that GeV optical transitions have a high quantum efficiency and are nearly lifetime broadened in such nanophotonic structures. These properties yield an efficient interface between waveguide photons and a single GeV center without the use of a cavity or slow-light waveguide. As a result, a single GeV center reduces waveguide transmission by $18 \pm 1\%$ on resonance in a single pass. We use a nanophotonic interferometer to perform homodyne detection of GeV resonance fluorescence. By probing the photon statistics of the output field, we demonstrate that the GeV–waveguide system is nonlinear at the single-photon level.

DOI: 10.1103/PhysRevLett.118.223603

Efficient coupling between single photons and coherent quantum emitters is a central element of quantum nonlinear optical systems and quantum networks [1–3]. Several atom-like defects in the solid state are currently being explored as promising candidates for the realization of such systems [4], including the nitrogen-vacancy (NV) center in diamond, renowned for its long spin coherence at room temperature [5], and the silicon-vacancy (SiV) center in diamond, which has recently been shown to have strong, coherent optical transitions in nanostructures [6–9]. The remarkable optical properties of the SiV center arise from its inversion symmetry [10], which results in a vanishing permanent electric dipole moment for SiV orbital states, dramatically reducing their response to charge fluctuations in the local environment. A large family of color centers in diamond is predicted to have inversion symmetry [11] and therefore may be expected to have similarly favorable optical properties. In this Letter, we demonstrate an efficient optical interface using negatively charged germanium-vacancy (GeV) color centers integrated into nanophotonic devices with optical properties that are superior to those of both NV and SiV centers. These properties result in high interaction probabilities between individual GeV centers and photons in a single-pass configuration, even without the use of cavities or other advanced photonic structures.

The GeV center is a new optically active color center in diamond [12–15]. Its calculated structure, shown in Fig. 1(a), is similar to that of the SiV center with D_{3d} symmetry [11,13]. The Ge impurity occupies an interstitial site between two vacancies along the $\langle 111 \rangle$ lattice direction [11,13,14], resulting in inversion symmetry. Figure 1(b) depicts the electronic level structure of the GeV center [13,14] with a zero-phonon line (ZPL) transition at 602 nm, which constitutes about 60% of the total emission spectrum [12]. Similar to the negatively charged SiV center [10,16], the ground state of the GeV center is a spin doublet ($S = 1/2$) [17] with double orbital degeneracy. The ground and excited orbital states of the GeV center are split by spin-orbit coupling, forming a four-level system visible in its cryogenic photoluminescence (PL) spectrum [Fig. 1(b)] [12,14,15]. As demonstrated in the complementary paper [17], this electronic structure allows one to directly control both orbital and electronic spin degrees of freedom using optical and microwave fields.

We achieve efficient coupling of individual GeV centers with single photons by incorporating them into

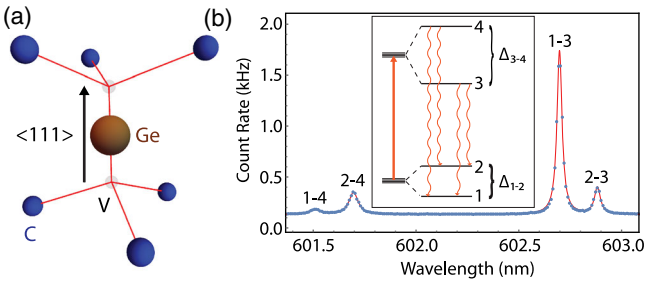

FIG. 1. (a) Molecular structure of the GeV center. (b) Photoluminescence spectrum of the GeV center at $T = 50$ K, revealing the four optical transitions predicted by the GeV electronic structure (inset) [12]. $\Delta_{1-2} = 152$ GHz and $\Delta_{3-4} = 981$ GHz are the measured ground- and excited-state orbital splittings, respectively. The solid curve is a fit to four Lorentzians.

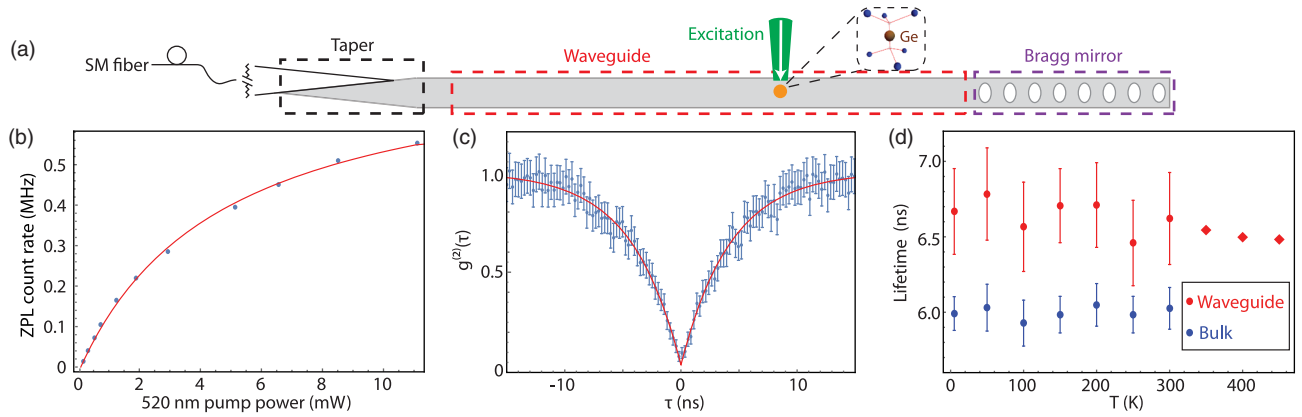

FIG. 2. (a) Schematic of a diamond nanophotonic device. Devices are 100 μm long and 480 nm wide and consist of a waveguide (red box), a partially reflective Bragg mirror (purple box), and a taper (black box) for coupling to a tapered single-mode (SM) fiber. (b) Saturation response for a single GeV center under continuous-wave, 520 nm excitation at $T = 300$ K, measured as a function of optical power at the microscope objective. The solid curve is a fit to a two-level saturation model [18]. (c) Intensity autocorrelation demonstrates antibunching of $g^{(2)}(0) = 0.08 \pm 0.02$. The solid curve is a single-exponential fit. (d) GeV center excited-state lifetime measurement at different temperatures in waveguides (red) and bulk diamond (blue). Error bars represent standard deviation of measured lifetimes of seven different emitters. For $T > 300$ K, the lifetime was measured for a single GeV center in a waveguide (red diamonds).

one-dimensional waveguides [Fig. 2(a)] with transverse dimensions on the order of the single-atom scattering cross section [7,19–21]. Waveguides have a width of 480 nm, and are nanofabricated from diamond [22,23]. GeV centers are incorporated into devices at low density using $^{74}Ge^{+}$ ion implantation ($10^{9}Ge^{+}$ cm^{-2}) and subsequent high temperature annealing at 1200 °C, leading to spatially resolvable single emitters [6,13]. We couple a single-mode tapered optical fiber to the waveguide with ~50% coupling efficiency by positioning it in contact with a tapered section of the diamond [7,23,24]. We implement this technique under a confocal microscope (described in Refs. [7,18]), enabling both free-space and fiber-based collection of fluorescence from GeV centers.

We first measure the ZPL emission of a single GeV center in a waveguide under continuous-wave 520 nm off-resonant excitation at room temperature [Fig. 2(b)]. Collecting via the tapered fiber, we observe a maximum single-photon detection rate of 0.56 ± 0.02 MHz on the narrow band ZPL around 602 nm, limited by excitation laser power. The single-photon nature of the emission is verified by antibunching of ZPL photons [Fig. 2(c)], measured at $I/I_{\mathrm{sat}} \sim 0.5$, where I and I_{sat} (4.7 ± 0.2 mW at 520 nm) are applied and saturation intensities, respectively. To better understand the optical properties of the GeV center, we measure its excited state lifetime at different temperatures with 532 nm pulsed excitation [Fig. 2(d)]. The GeV lifetime does not display significant temperature dependence up to $T = 450$ K, at which local vibrational modes with ~60 meV energy [12,14] have finite occupation ($\bar{n} \sim 0.27$). This demonstrates that multiphonon relaxation paths play a negligible role in determining the excited-state lifetime [25], suggesting a high radiative quantum efficiency. A statistically significant difference in lifetime for waveguide (6.6 ± 0.3 ns) and bulk (6.0 ± 0.1 ns) emitters implies a high sensitivity to the local photonic density of states [26–28], providing further evidence of a high radiative quantum efficiency.

To study coherence properties of single GeV centers in a waveguide, we use resonant excitation on transition 1–3 [Fig. 1(b)] at $T = 5$ K. We scan the frequency of the laser over the GeV resonance and record the fluorescence in the phonon sideband (PSB) collected into the tapered fiber. This technique yields a linewidth of 73 ± 1 MHz after 5 min of averaging at low excitation intensity [Fig. 3(a)]. The measured linewidth of a GeV center in a nanophotonic structure is within a factor of 3 of the lifetime-broadened limit, $\gamma_0/(2\pi) = 26 \pm 1$ MHz [18]. The measured linewidth increases with temperature up to $T = 300$ K [inset of Fig. 3(a)], due to phonon broadening that scales as $a + b(T - T_0)^3$ [$a = 0.0 \pm 0.2$ nm, $b = (1.9 \pm 0.5) \times 10^{-7}$ nmK^{-3}, $T_0 = (-13 \pm 23)$ K] for $T > 50$ K. The T^3 scaling suggests that optical coherence is limited by a two-phonon orbital relaxation process for $T > 50$ K, similar to the case of the SiV center [25].

In Fig. 3(b) we demonstrate coherent control over the GeV optical transition 1–3 by applying a resonant 40 ns pulse and observing optical Rabi oscillations using photons detected on the PSB. At high excitation power, the GeV optical transition undergoes spectral diffusion of roughly 300 MHz about the original resonance frequency. In order to mitigate spectral diffusion at high excitation intensities, we use an active feedback sequence [29,30] that stabilizes the GeV resonance frequency while maintaining a high duty cycle on resonance [18]. This procedure enables high contrast oscillations at a Rabi frequency of 310 ± 2 MHz with a decay time of 6.59 ± 0.02 ns at 5 K, close to the excited state lifetime of 6.1 ± 0.2 ns. The decay rate of Rabi oscillations increases linearly with temperature [inset in Fig. 3(b)], suggesting that a single-phonon orbital relaxation process limits optical coherence at low temperatures

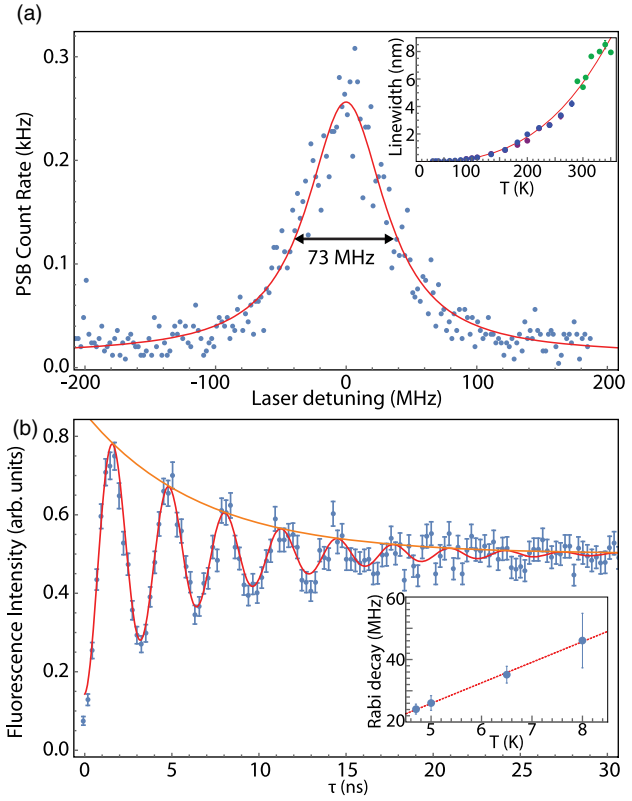

FIG. 3. (a) Transition 1–3 linewidth of a GeV center in a waveguide at $T = 5$ K, taken under resonant excitation at $I/I_{\mathrm{sat}} \sim 0.01$. The solid curve is a Lorentzian fit. Inset: Linewidth as a function of temperature; PL spectrum measured on a spectrometer under 520 nm excitation. Different colored points correspond to different emitters. The solid curve is a fit to a T^3 model [18]. (b) Optical Rabi oscillations. Fluorescence is measured on the PSB under resonant excitation. The solid curves are fits to a two-level model [18]. Inset: The Rabi oscillation decay rate scales linearly as a function of temperature for $T < 10$ K.

between $T = 5$ K and $T = 10$ K, again similar to the case of the SiV center [25].

These excellent optical properties allow us to observe the extinction of resonant transmission through a single GeV center in a waveguide, as demonstrated in Fig. 4. We focus the excitation on the Bragg mirror in order to scatter laser light into the waveguide. We collect the light transmitted through the GeV center into the tapered fiber, separating the transmitted and fluorescence (PSB) components using a bandpass filter [Fig. 4(a)]. We find that on resonance a single GeV center reduces waveguide transmission by $18 \pm 1\%$ [Fig. 4(b)]. The extinction of resonant light by a single quantum emitter is an effective measure of the strength of emitter-photon interactions, and is related to the emitter-waveguide cooperativity $C = \Gamma_{1D}/\Gamma'$, the ratio of the decay rate into the waveguide Γ_{1D} to the sum of atomic decay rates to all other channels and dephasing Γ' [19,20]. From the measured extinction from a single GeV center, we directly obtain the GeV–waveguide cooperativity of $C \geq 0.10 \pm 0.01$ [18]. Because the GeV center is a multilevel system with finite thermal population in level 2 at $T = 5$ K,

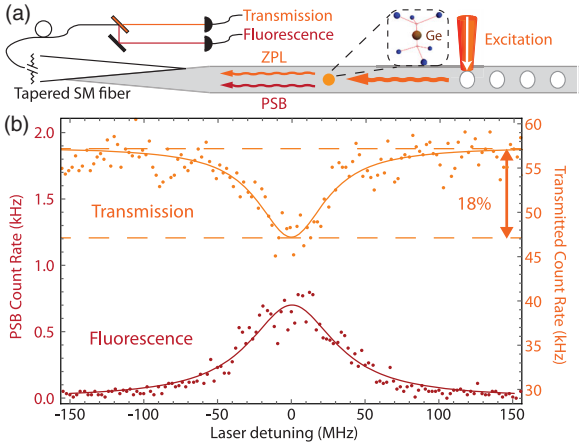

FIG. 4. (a) Schematic for single-pass transmission measurement. The resonant excitation ($I/I_{\mathrm{sat}} \sim 0.02$) is focused on the Bragg mirror to scatter light into the waveguide. We collect transmitted light into the tapered optical fiber and subsequently separate the transmission and fluorescence (PSB) using a bandpass filter. (b) Transmission spectrum of the GeV–waveguide device, showing $18 \pm 1\%$ extinction on resonance. Transmission is shown on top (right axis) in orange and PSB fluorescence is shown on the bottom (left axis) in red. The solid curves are Lorentzian fits.

the cooperativity extracted from transmission of light resonant with transition 1–3 is a lower bound and can be improved by initializing the GeV center in state 1 by optical pumping [7].

The extinction of resonant light results from destructive interference between the driving field (a local oscillator) and resonance fluorescence from the GeV center, and, in general, depends on the relative phase between them [31]. This phase can be controlled in a homodyne measurement involving a laser field and GeV resonance fluorescence in the stable nanophotonic interferometer depicted in Fig. 5(a). Here, the laser light is injected through one port of a fiber beam splitter connected to the tapered fiber and collected via a second beam splitter port. The reflected field at ZPL wavelengths consists of interference between GeV resonance fluorescence and the near-resonant excitation laser light reflected back into the fiber by the Bragg mirror, which acts as a local oscillator. We vary the relative amplitude and phase of the local oscillator with respect to the GeV resonance fluorescence by modifying the polarization of the input laser light (for details, see Ref. [18]). Using this technique, we observe the change in line shape of the output light from symmetric, corresponding to destructive interference (orange) to dispersive (blue) [Fig. 5(b)].

Finally, Fig. 5(c) demonstrates the quantum nonlinear character of the coupled GeV–waveguide system. In the homodyne measurement, the local oscillator is a weak coherent state with non-negligible single- and two-photon components, whereas the GeV resonance fluorescence consists of only single photons. In the case of large single atom-photon interaction probability, a single photon in the waveguide mode can saturate the GeV center and a single

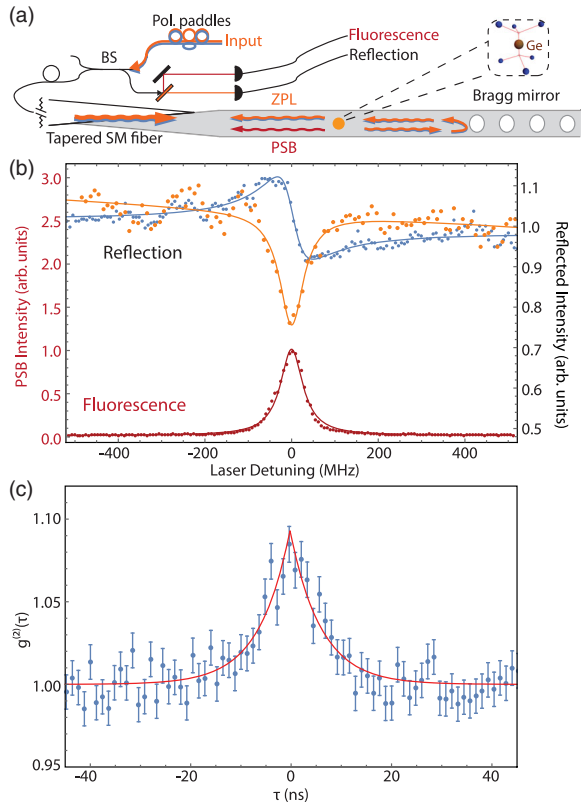

FIG. 5. (a) Schematic for homodyne interferometer. We excite ($I/I_{\mathrm{sat}} \sim 0.02$) and collect through two ports of a fiber beam splitter (BS). We use polarization paddles to change the excitation polarization. (b) Homodyne interfererometry with a single GeV center. The reflected signal is shown on top (right axis) at two different input polarizations (orange and blue). PSB fluorescence is shown on the bottom (left axis) in red. The solid red curve is a Lorentzian fit and the solid blue and orange curves are fits to a phenomenological model [18]. (c) Autocorrelation measurement. We perform Hanbury Brown–Twiss interferometry on the reflected field in the case of destructive interference for single photons. We measure bunching of $g^{(2)}(0) = 1.09 \pm 0.03$ with a decay time $\tau_b = 6.2 \pm 2.7$ ns. The solid curve is an exponential fit [18].

GeV center can alter the photon statistics of the output field [19]. As an example, in the case of destructive interference between the two fields, the output field consists preferentially of two-photon components from the local oscillator, resulting in photon bunching. We probe the photon statistics of the homodyne output field using Hanbury Brown–Twiss interferometry and observe, in the case of destructive interference, $g^{(2)}(0) = 1.09 \pm 0.03$ [Fig. 5(c)]. This observation provides direct evidence of device nonlinearity at the level of a single photon [7,19,21].

We now turn to the discussion of our experimental observations. The GeV excited state lifetime [Fig. 2(d)] sets a theoretical upper bound on the single-photon flux from a GeV center of roughly 160 MHz. From the saturation curve in Fig. 2(b), we infer that the maximum possible ZPL single-photon detection rate is 0.79 ± 0.02 MHz in our experiment. Accounting for the ZPL branching ratio and setup inefficiencies, we estimate that per excitation the probability of emission of a photon into the waveguide mode is at least 0.1 [18,28]. These measurements demonstrate that a single GeV center in a diamond waveguide is an efficient source of narrow band single photons.

The cooperativity measured in the transmission experiment (Fig. 4) is reduced by a combination of line-broadening mechanisms and multilevel dynamics [7,19]. Since the branching ratios of the GeV optical transitions are not yet known, it is difficult to develop a comprehensive model of the population dynamics. Using a simple three-level model, we estimate the phonon relaxation rate using $\gamma_p = 2\gamma_{\mathrm{Rabi}} - \frac{3}{2}\gamma_0$ [30], where γ_{Rabi} is the decay rate of Rabi oscillations and γ_0 (γ_p) is the excited-state (phonon) relaxation rate. Using the measured value of $\gamma_{\mathrm{Rabi}}/(2\pi) = 24 \pm 0.1$ MHz from Fig. 3(b), we infer that phonon relaxation leads to $\gamma_p/(2\pi) = 9 \pm 2$ MHz of Markovian line broadening at $T = 5$ K. Therefore, the observed 73 MHz linewidth is limited at 5 K by a combination of phonon relaxation and residual spectral diffusion and can likely be reduced further at lower temperatures, as demonstrated for GeV centers in bulk diamond [17].

The present observations, together with recent advances involving SiV centers [7], demonstrate significant potential for the realization of quantum nanophotonic devices using the family of color centers in diamond with inversion symmetry [11]. The negatively charged GeV center investigated here also has an electronic spin ($S = 1/2$) degree of freedom that can be manipulated using optical and microwave fields, making it a promising spin-photon interface [17]. As in the case of the SiV center, coherence between GeV orbital and spin sublevels is limited by phonon relaxation at finite temperatures. Ongoing efforts to suppress these relaxation processes at lower temperatures should result in long spin coherence times [25].

Our observations also point to some key differences in the optical properties of GeV and SiV centers. In particular, the GeV excited state lifetime [Fig. 2(d)] shows negligible temperature dependence and high sensitivity to changes in the local photonic density of states, indicating the primarily radiative nature of the decay. By contrast, the excited-state lifetime of the SiV center has strong temperature dependence [25] and does not respond as sensitively to changes in the local photonic density of states [6]. These observations demonstrate that the GeV center has a higher quantum efficiency than the SiV center and directly result in the strong extinction of light in a single pass, without the need for a slow-light waveguide or cavity. In particular, the large extinction observed from a single GeV center is competitive with single-pass transmission experiments using trapped atoms [32], ions [33], molecules [34], and quantum dots [35].

These observations open up exciting prospects for the realization of coherent quantum optical nodes with exceptionally strong atom-light coupling. In particular, the high quantum efficiency of the GeV center, when integrated into diamond nanocavities with previously demonstrated quality factor-mode volume ratios $Q/V > 10^4$ [22,23], could enable

device cooperativities $C > 100$, leading to deterministic single atom-photon interactions. GeV orbital and spin coherence properties can be improved by cooling devices below 1 K, potentially yielding long-lived quantum memories [25]. Arrays of such strongly coupled GeV–nanophotonic devices could be used as a basis for the realization of integrated quantum optical networks with applications in quantum information science [1] and studies of many-body physics with strongly interacting photons [3].

Financial support was provided by the NSF under Grant No. PHY-1506284, the Center for Ultracold Atoms under Grant No. PHY-1125846, the AFOSR MURI under Grant No. FA9550-16-1-0323, the ONR MURI, the DARPA QuINESS program, the ARL under Grant No. W911NF1520067, and the Vannevar Bush Faculty Fellowship program. F. J. is affiliated with the Center for Integrated Quantum Science and Technology (IQst) in BadenWürttemberg, Germany. Devices were fabricated at the Harvard CNS supported under NSF Grant No. ECS-0335765.

*mbhaskar@g.harvard.edu
†lukin@physics.harvard.edu

[1] H. J. Kimble, The quantum internet, Nature (London) **453**, 1023 (2008).
[2] P. Lodahl, S. Mahmoodian, and S. Stobbe, Interfacing single photons and single quantum dots with photonic nanostructures, Rev. Mod. Phys. **87**, 347 (2015).
[3] I. Carusotto and C. Ciuti, Quantum fluids of light, Rev. Mod. Phys. **85**, 299 (2013).
[4] I. Aharonovich, D. Englund, and M. Toth, Solid-state single-photon emitters, Nat. Photonics **10**, 631 (2016).
[5] P. C. Maurer, G. Kucsko, C. Latta, L. Jiang, N. Y. Yao, S. D. Bennett, F. Pastawski, D. Hunger, N. Chisholm, M. Markham *et al.*, Room-temperature quantum bit memory exceeding one second, Science **336**, 1283 (2012).
[6] R. E. Evans, A. Sipahigil, D. D. Sukachev, A. S. Zibrov, and M. D. Lukin, Narrow-Linewidth Homogeneous Optical Emitters in Diamond Nanostructures via Silicon Ion Implantation, Phys. Rev. Applied **5**, 044010 (2016).
[7] A. Sipahigil, R. E. Evans, D. D. Sukachev, M. J. Burek, J. Borregaard, M. K. Bhaskar, C. T. Nguyen, J. L. Pacheco, H. A. Atikian, C. Meuwly *et al.*, An integrated diamond nanophotonics platform for quantum-optical networks, Science **354**, 847 (2016).
[8] U. Jantzen, A. B. Kurz, D. S. Rudnicki, C. Schäfermeier, K. D. Jahnke, U. L. Andersen, V. A. Davydov, V. N. Agafonov, A. Kubanek, L. J. Rogers, and F. Jelezko, Nanodiamonds carrying silicon-vacancy quantum emitters with almost lifetime-limited linewidths, New J. Phys. **18**, 073036 (2016).
[9] K. Li, Y. Zhou, A. Rasmita, I. Aharonovich, and W. B. Gao, Nonblinking Emitters with Nearly Lifetime-Limited Linewidths in CVD Nanodiamonds, Phys. Rev. Applied **6**, 024010 (2016).
[10] C. Hepp, T. Müller, V. Waselowski, J. N. Becker, B. Pingault, H. Sternschulte, D. Steinmüller-Nethl, A. Gali, J. R. Maze, M. Atatüre, and C. Becher, Electronic Structure of the Silicon Vacancy Color Center in Diamond, Phys. Rev. Lett. **112**, 036405 (2014).
[11] J. P. Goss, P. R. Briddon, M. J. Rayson, S. J. Sque, and R. Jones, Vacancy-impurity complexes and limitations for implantation doping of diamond, Phys. Rev. B **72**, 035214 (2005).
[12] Y. N. Palyanov, I. N. Kupriyanov, Y. M. Borzdov, and N. V. Surovtsev, Germanium: A new catalyst for diamond synthesis and a new optically active impurity in diamond, Sci. Rep. **5**, 14789 (2015).
[13] T. Iwasaki, F. Ishibashi, Y. Miyamoto, Y. Doi, S. Kobayashi, T. Miyazaki, K. Tahara, K. D. Jahnke, L. J. Rogers, B. Naydenov *et al.*, Germanium-vacancy single color centers in diamond, Sci. Rep. **5**, 12882 (2015).
[14] E. A. Ekimov, S. Lyapin, K. N. Boldyrev, M. V. Kondrin, R. Khmelnitskiy, V. A. Gavva, T. V. Kotereva, and M. N. Popova, Germanium-vacancy color center in isotopically enriched diamonds synthesized at high pressures, JETP Lett. **102**, 701 (2015).
[15] Y. N. Palyanov, I. N. Kupriyanov, Y. M. Borzdov, A. F. Khokhryakov, and N. V. Surovtsev, High-pressure synthesis and characterization of Ge-doped single crystal diamond, Cryst. Growth Des. **16**, 3510 (2016).
[16] T. Müller, C. Hepp, B. Pingault, E. Neu, S. Gsell, M. Schreck, H. Sternschulte, D. Steinmüller-Nethl, C. Becher, and M. Atatüre, Optical signatures of silicon-vacancy spins in diamond, Nat. Commun. **5**, 3328 (2014).
[17] P. Siyushev, M. H. Metsch, A. Ijaz, J. M. Binder, M. K. Bhaskar, D. D. Sukachev, A. Sipahigil, R. E. Evans, C. T. Nguyen, M. D. Lukin *et al.*, Optical and microwave control of germanium-vacancy center spins in diamond, arXiv:1612.02947.
[18] See Supplemental Material at http://link.aps.org/supplemental/10.1103/PhysRevLett.118.223603 for details about the experimental setup, the GeV–waveguide coupling efficiency, fits to data in the main text, calculation of cooperativity, and operating principles of homodyne measurement.
[19] D. E. Chang, A. S. Sørensen, E. A. Demler, and M. D. Lukin, A single-photon transistor using nanoscale surface plasmons, Nat. Phys. **3**, 807 (2007).
[20] A. Goban, C. L. Hung, J. D. Hood, S. P. Yu, J. A. Muniz, O. Painter, and H. J. Kimble, Superradiance for Atoms Trapped along a Photonic Crystal Waveguide, Phys. Rev. Lett. **115**, 063601 (2015).
[21] A. Javadi, I. Söllner, M. Arcari, S. L. Hansen, L. Midolo, S. Mahmoodian, G. Kiršanskė, T. Pregnolato, E. Lee, J. Song *et al.*, Single-photon nonlinear optics with a quantum dot in a waveguide, Nat. Commun. **6**, 8655 (2015).
[22] M. J. Burek, Y. Chu, M. S. Liddy, P. Patel, J. Rochman, S. Meesala, W. Hong, Q. Quan, M. D. Lukin, and M. Lončar, High quality-factor optical nanocavities in bulk single-crystal diamond, Nat. Commun. **5**, 5718 (2014).
[23] M. J. Burek, C. Meuwly, R. E. Evans, M. K. Bhaskar, A. Sipahigil, S. Meesala, D. D. Sukachev, C. T. Nguyen, J. L. Pacheco, E. Bielejec *et al.*, A fiber-coupled diamond quantum nanophotonic interface, arXiv:1612.05285.
[24] T. G. Tiecke, K. P. Nayak, J. D. Thompson, T. Peyronel, N. P. de Leon, V. Vuletić, and M. D. Lukin, Efficient fiber-optical interfaces for nanophotonic devices, Optica **2**, 70 (2015).

[25] K. D. Jahnke, A. Sipahigil, J. M. Binder, M. W. Doherty, M. Metsch, L. J. Rogers, N. B. Manson, M. D. Lukin, and F. Jelezko, Electron-phonon processes of the silicon-vacancy centre in diamond, New J. Phys. **17**, 043011 (2015).

[26] A. Khalid, K. Chung, R. Rajasekharan, D. W. Lau, T. J. Karle, B. C. Gibson, and S. Tomljenovic-Hanic, Lifetime reduction and enhanced emission of single photon color centers in nanodiamonds via surrounding refractive index modification, Sci. Rep. **5**, 11179 (2015).

[27] M. Frimmer, A. Mohtashami, and A. Femius Koenderink, Nanomechanical method to gauge emission quantum yield applied to nitrogen-vacancy centers in nanodiamond, Appl. Phys. Lett. **102**, 121105 (2013).

[28] R. N. Patel, T. Schröder, N. Wan, L. Li, S. L. Mouradian, E. H. Chen, and D. R. Englund, Efficient photon coupling from a diamond nitrogen vacancy center by integration with silica fiber, Light Sci. Appl. **5**, e16032 (2016).

[29] H. Bernien, B. Hensen, W. Pfaff, G. Koolstra, M. S. Blok, L. Robledo, T. H. Taminiau, M. Markham, D. J. Twitchen, L. Childress, and R. Hanson, Heralded entanglement between solid-state qubits separated by three metres, Nature (London) **497**, 86 (2013).

[30] M. L. Goldman, A. Sipahigil, M. W. Doherty, N. Y. Yao, S. D. Bennett, M. Markham, D. J. Twitchen, N. B. Manson, A. Kubanek, and M. D. Lukin, Phonon-Induced Population Dynamics and Intersystem Crossing in Nitrogen-Vacancy Centers, Phys. Rev. Lett. **114**, 145502 (2015).

[31] C. H. Schulte, J. Hansom, A. E. Jones, C. Matthiesen, C. Le Gall, and M. Atatüre, Quadrature squeezed photons from a two-level system, Nature (London) **525**, 222 (2015).

[32] M. K. Tey, Z. Chen, S. A. Aljunid, B. Chng, F. Huber, G. Maslennikov, and C. Kurtsiefer, Strong interaction between light and a single trapped atom without the need for a cavity, Nat. Phys. **4**, 924 (2008).

[33] G. Hétet, L. Slodička, M. Hennrich, and R. Blatt, Single atom as a mirror of an optical cavity, Phys. Rev. Lett. **107**, 133002 (2011).

[34] G. Wrigge, I. Gerhardt, J. Hwang, G. Zumofen, and V. Sandoghdar, Efficient coupling of photons to a single molecule and the observation of its resonance fluorescence, Nat. Phys. **4**, 60 (2008).

[35] A. N. Vamivakas, M. Atatüre, J. Dreiser, S. T. Yilmaz, A. Badolato, A. K. Swan, B. B. Goldberg, A. Imamoglu, and M. S. Ünlü, Strong extinction of a far-field laser beam by a single quantum dot, Nano Lett. **7**, 2892 (2007).